Electronic Supplementary Material (ESI) for Physical Chemistry Chemical Physics.

Supporting Information
A perspective on the relative merits/demerits of time-propagators based on Floquet theorem

Shreyan Ganguly and Ramesh Ramachandran*
Department of Chemical Sciences

Indian Institute of Science Education and Research (IISER) Mohali, Sector 81,Manauli P.O. Box-140306, Mohali, Punjab, India

*Author to whom correspondence should be addressed: rramesh@iisermohali.ac.in

Part-A (Method-I)

A1. Time evolution in the Schrödinger picture

As the operator $\overline{H}$ has off diagonal operators, an additional transformation is performed on the $\overline{H}$ operator (resulting in a transformed operator, $\overline{H_d}$, which is diagonal in the Hilbert space) and is defined in terms of the polarization operator basis as follows:

$$U_1 = e^{i\theta_\beta I_X S_\beta} e^{i\theta_\alpha I_X S_\alpha} \tag{1}$$

$$\tan\theta_{\alpha/\beta} = \frac{\left(\omega_I^{(Y)} \pm 2\omega_{IS}^{(Y)}\right)}{\omega_I^{(Z)}} \tag{2}$$

$$\overline{H_d} = U_1 \overline{H} U_1^\dagger = \tilde{\omega}_I^{(Z)} I_Z + \tilde{\omega}_{IS}^{(Z)} I_Z S_Z \tag{3}$$

where $S_{\alpha/\beta} = \left(\frac{1}{2}\right) \pm S_Z$ are the polarization operators for the 'S'-spin. For the purpose of the discussion in this section we have also considered on-resonance CW irradiation (i.e. set the offset on the 'I'-spin ($\Delta\omega$) as zero). The coefficients $\tilde{\omega}_I^{(Z)}/\tilde{\omega}_{IS}^{(Z)}$ are defined in terms of the original ω-coefficients in the operator $\overline{H}$ (Eq.(90) of the main section).

$$\tilde{\omega}_I^{(Z)} = -\left[\left(\frac{\omega_I^{(Z)}}{2}\right)^2 + \left(\frac{\omega_I^{(Y)}}{2} + \omega_{IS}^{(Y)}\right)^2\right]^{1/2} - \left[\left(\frac{\omega_I^{(Z)}}{2}\right)^2 + \left(\frac{\omega_I^{(Y)}}{2} - \omega_{IS}^{(Y)}\right)^2\right]^{1/2} \tag{4}$$

$$\tilde{\omega}_{IS}^{(Z)} = -\left(\frac{1}{2}\right)\left[\left(\frac{\omega_I^{(Z)}}{2}\right)^2 + \left(\frac{\omega_I^{(Y)}}{2} + \omega_{IS}^{(Y)}\right)^2\right]^{1/2} + \left(\frac{1}{2}\right)\left[\left(\frac{\omega_I^{(Z)}}{2}\right)^2 + \left(\frac{\omega_I^{(Y)}}{2} - \omega_{IS}^{(Y)}\right)^2\right]^{1/2} \tag{5}$$

To maintain consistency, both the initial density operator ($\rho(0) = S_X$), the operator, $P(t)$ and the detection operator, S^+ are also transformed as follows.

$$\rho_d(0) = U_1 \rho(0) U_1^\dagger = S_X \cos\left(\frac{\theta_\alpha - \theta_\beta}{2}\right) - 2I_X S_Y \sin\left(\frac{\theta_\alpha - \theta_\beta}{2}\right) \tag{6}$$

$$P_d(t) = U_1 P(t) U_1^\dagger \simeq P(t) \tag{7}$$

$$S_d^+ = U_1 S^+ U_1^\dagger = S^+ \cos\left(\frac{\theta_\alpha - \theta_\beta}{2}\right) + 2iI_X S^+ \sin\left(\frac{\theta_\alpha - \theta_\beta}{2}\right) \tag{8}$$

where we have retained the corrections due to the transformations for the operator $P(t)$ to the lowest order.

Employing the above relations, the time-domain signal can be derived through suitable approximations as follows.

$$\rho_d(t) = U_d(t)\,\rho_d(0)\,U_d^\dagger(t) = P_d(t)\,e^{-i\overline{H_d}t}\rho_d(0)\,e^{i\overline{H_d}t}P_d^\dagger(t) \tag{9}$$

where, $U_d(t) = U_1 U(t) U_1^\dagger = P_d(t)\,e^{-i\overline{H_d}t}$, represents the transformed evolution operator.

$$\rho_d(t) = P_d(t)\underbrace{e^{-i\overline{H_d}t}\rho_d(0)\,e^{i\overline{H_d}t}}_{\rho_d'(t)}P_d^\dagger(t) = \{P_0(t) + P_1(t) + P_2(t)\}\,\rho_d'(t)\left\{P_0^\dagger(t) + P_1^\dagger(t) + P_2^\dagger(t)\right\} \tag{10}$$

By employing the form of $\overline{H_d}$ given above, the form for $\rho'_d(t)$ can be derived as follows.

$$\rho'_d(t) = \cos\left(\frac{\theta_\alpha - \theta_\beta}{2}\right)\left\{S_X \cos\left(\frac{\tilde{\omega}_{IS}^{(Z)} t}{2}\right) + 2I_Z S_Y \sin\left(\frac{\tilde{\omega}_{IS}^{(Z)} t}{2}\right)\right\}$$
$$- 2\sin\left(\frac{\theta_\alpha - \theta_\beta}{2}\right)\left\{I_X S_Y \cos\left(\tilde{\omega}_I^{(Z)} t\right) + I_Y S_Y \sin\left(\tilde{\omega}_I^{(Z)} t\right)\right\} \quad (11)$$

This leads to the following form for the signal expression:

$$S(t) = Tr\left[\rho_d(t) S_d^+\right] = C_1(t).\cos\left(\frac{\tilde{\omega}_{IS}^{(Z)} t}{2}\right) + S_1(t).\sin\left(\frac{\tilde{\omega}_{IS}^{(Z)} t}{2}\right)$$
$$+ C_2(t).\cos\left(\tilde{\omega}_I^{(Z)} t\right) + S_2(t).\sin\left(\tilde{\omega}_I^{(Z)} t\right) \quad (12)$$

where the coefficients $C_i(t)/S_i(t)$ are defined in Table 1.

CW Decoupling Method-I	**Signal Coefficient**
$C_1(t)$	$\left\{\frac{1}{2}C_{id}(t)C_Z^*(t)-\frac{1}{2}C_Z(t)C_{id}^*(t)\right\}\cos^2\left(\frac{\theta_\alpha-\theta_\beta}{2}\right)$ $+\left\{\frac{1}{8}C_X(t)C_{XZ}^*(t)-\frac{1}{8}C_{XZ}(t)C_X^*(t)+\frac{1}{8}C_{YZ}(t)C_Y^*(t)-\frac{1}{8}C_Y(t)C_{YZ}^*(t)\right\}\cos^2\left(\frac{\theta_\alpha-\theta_\beta}{2}\right)$ $+\left\{C_{id}(t)C_{id}^*(t)+\frac{1}{4}C_X(t)C_X^*(t)+\frac{1}{4}C_Y(t)C_Y^*(t)+\frac{1}{4}C_Z(t)C_Z^*(t)\right\}\cos^2\left(\frac{\theta_\alpha-\theta_\beta}{2}\right)$ $+\left\{\frac{1}{16}C_{XZ}(t)C_{XZ}^*(t)+\frac{1}{16}C_{YZ}(t)C_{YZ}^*(t)\right\}\cos^2\left(\frac{\theta_\alpha-\theta_\beta}{2}\right)$ $+\left(\frac{i}{4}\right)\left\{C_{id}(t)C_X^*(t)+C_X(t)C_{id}^*(t)+\frac{1}{4}C_X(t)C_{XZ}^*(t)+\frac{1}{4}C_{XZ}(t)C_X^*(t)\right\}\sin(\theta_\alpha-\theta_\beta)$ $-\left(\frac{1}{2}\right)\left\{-\frac{i}{4}C_{id}(t)C_{XZ}^*(t)+\frac{i}{2}C_{XZ}(t)C_{id}^*(t)+\frac{i}{2}C_Z(t)C_X^*(t)-\frac{i}{2}C_X(t)C_Z^*(t)\right\}\sin(\theta_\alpha-\theta_\beta)$
$S_1(t)$	$-\left(\frac{1}{2}\right)\left\{-\frac{i}{2}C_{id}(t)C_Y^*(t)+\frac{i}{2}C_Y(t)C_{id}^*(t)\right\}\sin(\theta_\alpha-\theta_\beta)$ $+\left(\frac{i}{2}\right)\left\{\frac{1}{4}C_{id}(t)C_{YZ}^*(t)-\frac{1}{4}C_{YZ}(t)C_{id}^*(t)\right\}\sin(\theta_\alpha-\theta_\beta)$
$C_2(t)$	$-\left\{\frac{i}{8}C_X(t)C_Z^*(t)-\frac{i}{8}C_Z(t)C_X^*(t)\right\}\sin(\theta_\alpha-\theta_\beta)$ $-\left\{\frac{i}{4}C_{id}(t)C_X^*(t)+\frac{i}{4}C_X(t)C_{id}^*(t)\right\}\sin(\theta_\alpha-\theta_\beta)$ $+\frac{1}{2}\left\{C_{id}(t)C_{id}^*(t)+\frac{1}{4}C_X(t)C_X^*(t)-\frac{1}{4}C_Y(t)C_Y^*(t)-\frac{1}{4}C_Z(t)C_Z^*(t)\right\}\sin^2\left(\frac{\theta_\alpha-\theta_\beta}{2}\right)$ $+\left\{-\frac{1}{16}C_{XZ}(t)C_{XZ}^*(t)+\frac{1}{16}C_{YZ}(t)C_{YZ}^*(t)\right\}\sin^2\left(\frac{\theta_\alpha-\theta_\beta}{2}\right)$ $-(i)\left\{\frac{i}{2}C_{id}(t)C_Z^*(t)-\frac{i}{2}C_Z(t)C_{id}^*(t)\right\}\sin\left(\frac{\theta_\alpha-\theta_\beta}{2}\right)$ $-(i)\left\{\frac{i}{8}C_X(t)C_{XZ}^*(t)-\frac{i}{8}C_{XZ}(t)C_X^*(t)\right\}\sin\left(\frac{\theta_\alpha-\theta_\beta}{2}\right)$ $-(i)\left\{-\frac{i}{8}C_Y(t)C_{YZ}^*(t)-\frac{i}{8}C_{YZ}(t)C_Y^*(t)\right\}\sin\left(\frac{\theta_\alpha-\theta_\beta}{2}\right)$
$S_2(t)$	$-\left\{\frac{i}{8}C_{id}(t)C_{YZ}^*(t)-\frac{i}{8}C_{YZ}(t)C_{id}^*(t)\right\}\sin(\theta_\alpha-\theta_\beta)$ $-\left\{\frac{i}{4}C_{id}(t)C_Y^*(t)-\frac{i}{4}C_Y(t)C_{id}^*(t)\right\}\sin(\theta_\alpha-\theta_\beta)$ $+\left\{\frac{1}{4}C_X(t)C_Y^*(t)+\frac{1}{4}C_Y(t)C_X^*(t)-\frac{1}{16}C_{XZ}(t)C_{YZ}^*(t)-\frac{1}{16}C_{YZ}(t)C_{XZ}^*(t)\right\}\sin^2\left(\frac{\theta_\alpha-\theta_\beta}{2}\right)$ $-(i)\left\{\frac{i}{8}C_X(t)C_{YZ}^*(t)-\frac{i}{8}C_{YZ}(t)C_X^*(t)+\frac{i}{8}C_Y(t)C_{YZ}^*(t)-\frac{i}{8}C_{XZ}(t)C_Y^*(t)\right\}\sin^2\left(\frac{\theta_\alpha-\theta_\beta}{2}\right)$

Table 1: Description of coefficients ($C_i(t)$ and $S_i(t)$) appearing in the derivation of the time-domain signal (Eq.(12)) based on Method-I (Schrödinger picture formalism)

Role of non-secular terms in time evolution

To rule out the role of the non-secular terms (such $[\mathcal{H}_0, \mathcal{H}_n]$) in $\overline{H}$ in the discrepancy observed in the analytic simulations in the Schrödinger picture, additional simulations, both in the presence and absence of the non-secular terms were performed and compared with numerical simulations. As indicated in Figure 1, the analytic simulations both in the presence (first row, indicated in red color) and absence (second row, indicated in blue color) are in complete disagreement to those obtained from numerical simulations (indicated in black color). Hence, the disagreement observed in the analytic simulations could be due to some inherent limitations of the method.

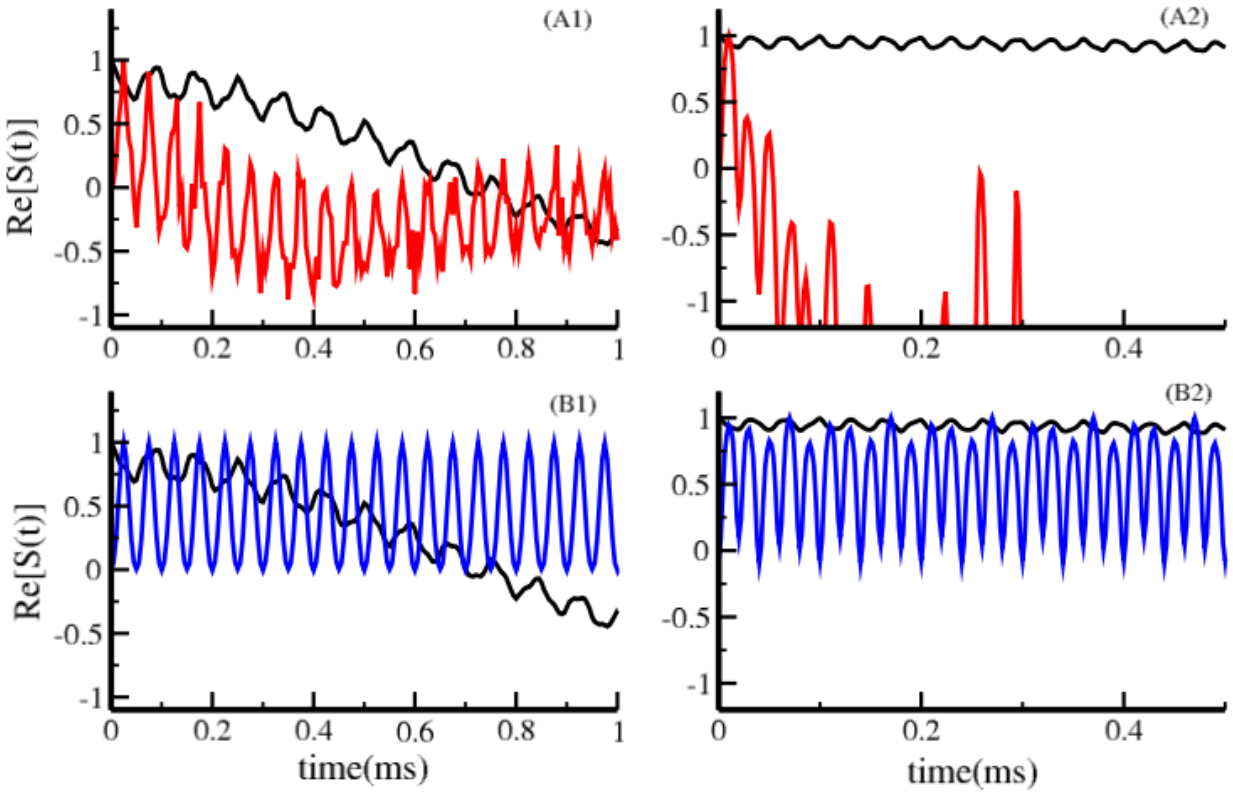

Figure 1: In the simulations depicted, the time-domain signal (panels A1, A2 and B1, B2) under CW decoupling is illustrated under varying spinning frequencies and RF amplitudes (i.e. $\nu_r = 20$ kHz; $\nu_1 = 50$ kHz (panels A1, B1) and $\nu_r = 50$ kHz; $\nu_1 = 20$ kHz (panels A2, B2)). The simulations from numerical methods (indicated through black solid line) are compared with analytic simulations based on **single-mode** based Method-I formalism with i) complete form of $\overline{H}$ (indicated in red, top row) and ii) with non-secular terms dropped from $\overline{H}$ (indicated in blue, bottom row). All other parameters are similar to those employed in the main article.

A2. Time evolution in the Interaction picture

(i) Normal boundary condition ($P(0) = 1$)

Based on the calculations given in the main section, the final form of the signal expression in the interaction picture is given by the following equation.

$$S(t) = Tr\left[\rho(t) S^{+}\right] = C_1(t).\cos\left(\frac{\tilde{\omega}_{IS}^{(Z)} t}{2}\right) + S_1(t).\sin\left(\frac{\tilde{\omega}_{IS}^{(Z)} t}{2}\right) \tag{13}$$

where the coefficients $C_i(t)/S_i(t)$ are defined in Table 2.

CW Decoupling Method-I	**Signal Coefficient**
$C_1(t)$	$1+\left(\frac{1}{2}\right)\{C^*_{PM}(t)+C^*_{MP}(t)+C_{PM}(t)+C_{MP}(t)\}$ $+\left(\frac{1}{4}\right)\{C^*_{PMZ}(t)+C^*_{MPZ}(t)-C_{PMZ}(t)-C_{MPZ}(t)\}$ $\left(\frac{1}{2}\right)\{C_P(t)C^*_P(t)+C_M(t)C^*_M(t)\}++\left(\frac{1}{4}\right)\{C_P(t)C^*_{PZ}(t)+C_M(t)C^*_{MZ}(t)\}$ $-\left(\frac{1}{4}\right)\{C_{PZ}(t)C^*_P(t)+C_{MZ}(t)C^*_M(t)\}-\left(\frac{1}{8}\right)\{C_{PZ}(t)C^*_{PZ}(t)+C_{MZ}(t)C^*_{MZ}(t)\}$
$S_1(t)$	$\left(\frac{i}{2}\right)\{C^*_{PM}(t)-C^*_{MP}(t)+C_{PM}(t)-C_{MP}(t)\}$ $\left(\frac{i}{4}\right)\{C^*_{PMZ}(t)-C^*_{PMZ}(t)-C_{PMZ}(t)+C_{MPZ}(t)\}$ $-\left(\frac{i}{2}\right)\{C_P(t)C^*_P(t)-C_M(t)C^*_M(t)\}-\left(\frac{i}{4}\right)\{C_P(t)C^*_{PZ}(t)-C_M(t)C^*_{MZ}(t)\}$ $\left(\frac{i}{4}\right)\{C_{PZ}(t)C^*_P(t)-C_{MZ}(t)C^*_M(t)\}+\left(\frac{i}{8}\right)\{C_{PZ}(t)C^*_{PZ}(t)-C_{MZ}(t)C^*_{MZ}(t)\}$

Table 2: Description of coefficients ($C_i(t)$ and $S_i(t)$) appearing in the derivation of the time-domain signal (Eq.(96) of the main article) based on Method-I (Interaction picture formalism)

(ii) Alternate boundary condition ($P(0) \neq 1$)

Employing the bimodal framework, the evolution operator in the standard Hilbert space is derived in terms of the operators $\overline{H}$ and $P(t)$, as given below.

$$U(t) = P(t)\, e^{-i\overline{H}t} P^{\dagger}(0) \tag{14}$$

$$\overline{H} = \overline{H}^{(0)} + \overline{H}^{(1)} + \overline{H}^{(2)} = \underbrace{\tilde{\omega}_I^{(Z)} I_Z + \tilde{\omega}_{IS}^{(Z)} I_Z S_Z}_{\overline{H}^{(2)}} \tag{15}$$

$$\begin{aligned} P(t) &= P_0(t) + P_1(t) + P_2(t) \\ &= \underbrace{\mathbb{1}}_{P_0(t)} + \underbrace{C_P(t) I^+ + C_M(t) I^- + C_{PZ}(t) I^+ S_Z + C_{MZ}(t) I^- S_Z}_{P_1(t)} \\ &+ \underbrace{C_{PM}(t) I^+ I^- + C_{MP}(t) I^- I^+ + C_{PMZ}(t) I^+ I^- S_Z + C_{MPZ}(t) I^- I^+ S_Z}_{P_2(t)} \end{aligned} \tag{16}$$

A detailed description of the various cross-terms employed in the derivation of the effective evolution operator is listed in Table 3.

Subsequently, utilizing the modified form of $U(t)$, the evolution of the system under CW decoupling is calculated and given below.

$$\rho(t) = U(t)\, \rho(0)\, U^{\dagger}(t) = P(t)\, e^{-i\overline{H}t} P^{\dagger}(0)\, \rho(0)\, P(0)\, e^{i\overline{H}t} P^{\dagger}(t) \tag{17}$$

$$\begin{aligned} \rho(t) &= P(t) \underbrace{e^{-i\overline{H}t} P^{\dagger}(0)\, \rho(0)\, P(0)\, e^{i\overline{H}t}}_{\tilde{\rho}_0(t)} P^{\dagger}(t) \\ &= \left[P_0(t) + P_1(t) + P_2(t)\right] \tilde{\rho}_0(t) \left[P_0^{\dagger}(t) + P_1^{\dagger}(t) + P_2^{\dagger}(t)\right] \end{aligned} \tag{18}$$

where,

$$\begin{aligned} \tilde{\rho}_0(0) &= P^{\dagger}(0)\, \rho(0)\, P(0) = \left[P_0^{\dagger}(0) + P_1^{\dagger}(0) + P_2^{\dagger}(0)\right] \rho(0) \left[P_0(0) + P_1(0) + P_2(0)\right] \\ &= A_X(0) S_X + A_{PX}(0) I^+ S_X + A_{MX}(0) I^- S_X + A_{PY}(0) I^+ S_Y + A_{MY}(0) I^- S_Y \\ &+ A_{PMX}(0) I^+ I^- S_X + A_{MPX}(0) I^- I^+ S_X + A_{PMY}(0) I^+ I^- S_Y + A_{MPY}(0) I^- I^+ S_Y \end{aligned} \tag{19}$$

Cross-Term (CW Decoupling)	**Method-I (bimodal)**	**Method-I (bimodal)**
Operator	$\overline{\boldsymbol{H}}$	$\boldsymbol{P}\left(\boldsymbol{t}\right)$
$\mathrm{H_I}$	-	$\left\{\sum\limits_{m=-2}^{2}\left(\frac{\omega_I^{(m)}}{2(m\omega_r\pm\omega_1)}\right)e^{i(m\omega_r\pm\omega_1)t}\right\}I^{\pm}\equiv C_{P/M}\left(t\right)I^{\pm}$
$\mathrm{H_{IS}}$	-	$\left\{\sum\limits_{\substack{m=-2\\m\neq0}}^{2}\left(\frac{\omega_{IS}^{(m)}}{(m\omega_r\pm\omega_1)}\right)e^{i(m\omega_r\pm\omega_1)t}\right\}I^{\pm}S_Z\equiv C_{PZ/MZ}\left(t\right)I^{\pm}S_Z$
$\mathrm{H_I}\times\mathrm{H_I}$	$-\frac{1}{2}\left\{\sum\limits_{m=-2}^{2}\frac{\left\lvert\omega_I^{(m)}\right\rvert^2\omega_1}{\left(m^2\omega_r^2-\omega_1^2\right)}\right\}I_Z\equiv\tilde{\omega}_I^{(Z)}I_Z$	$\left(\frac{1}{4}\right)\left[\sum\limits_{\substack{m,m'=-2\\m+m'\neq0}}^{2}\left(\frac{e^{i(m+m')\omega_r t}}{(m+m')\omega_r}\right)\left\{\frac{\omega_I^{(m)}\omega_I^{(m')}}{(m'\omega_r\mp\omega_1)}\right\}\right]I^{\pm}I^{\mp}$ $-\left(\frac{1}{4}\right)\left[\sum\limits_{\substack{m,m'=-2\\m+m'\neq0}}^{2}\left(e^{i(m\omega_r\pm\omega_1)t}\right)\left\{\frac{\omega_I^{(m)}\omega_I^{(m')}}{(m\omega_r\mp\omega_1)(m'\omega_r\mp\omega_1)}\right\}\right]I^{\pm}I^{\mp}\equiv C_{PM/MP}\left(t\right)I^{\pm}I^{\mp}$
$\mathrm{H_{IS}}\times\mathrm{H_{IS}}$	$-\frac{1}{2}\left\{\sum\limits_{\substack{m=-2\\m\neq0}}^{2}\frac{\left\lvert\omega_{IS}^{(m)}\right\rvert^2\omega_1}{\left(m^2\omega_r^2-\omega_1^2\right)}\right\}I_Z\equiv\tilde{\omega}_I^{(Z)}I_Z$	$\left(\frac{1}{4}\right)\left[\sum\limits_{\substack{m,m'=-2\\m+m'\neq0}}^{2}\left(\frac{e^{i(m+m')\omega_r t}}{(m+m')\omega_r}\right)\left\{\frac{\omega_{IS}^{(m)}\omega_{IS}^{(m')}}{(m'\omega_r\mp\omega_1)}\right\}\right]I^{\pm}I^{\mp}$ $-\left(\frac{1}{4}\right)\left[\sum\limits_{\substack{m,m'=-2\\m+m'\neq0}}^{2}\left(e^{i(m\omega_r\pm\omega_1)t}\right)\left\{\frac{\omega_{IS}^{(m)}\omega_{IS}^{(m')}}{(m\omega_r\mp\omega_1)(m'\omega_r\mp\omega_1)}\right\}\right]I^{\pm}I^{\mp}\equiv C_{PM/MP}\left(t\right)I^{\pm}I^{\mp}$
$\mathrm{H_I}\times\mathrm{H_{IS}}$	$-\left\{\sum\limits_{m=-2}^{2}\left(\omega_I^{(m)}\omega_{IS}^{(-m)}+\omega_{IS}^{(m)}\omega_I^{(-m)}\right)\underbrace{\frac{\omega_1}{\left(m^2\omega_r^2-\omega_1^2\right)}}_{\text{ResDip}}\right\}I_ZS_Z$ $\equiv\tilde{\omega}_{IS}^{(Z)}I_ZS_Z$	$\left(\frac{1}{2}\right)\left[\sum\limits_{\substack{m,m'=-2\\m+m'\neq0}}^{2}\left(\frac{e^{i(m+m')\omega_r t}}{(m+m')\omega_r}\right)\left\{\frac{\omega_I^{(m)}\omega_{IS}^{(m')}+\omega_{IS}^{(m)}\omega_I^{(m')}}{(m'\omega_r\mp\omega_1)}\right\}\right]I^{\pm}I^{\mp}S_Z$ $-\left(\frac{1}{2}\right)\left[\sum\limits_{\substack{m,m'=-2\\m+m'\neq0}}^{2}\left(e^{i(m\omega_r\pm\omega_1)t}\right)\left\{\frac{\omega_I^{(m)}\omega_{IS}^{(m')}+\omega_{IS}^{(m)}\omega_I^{(m')}}{(m\omega_r\mp\omega_1)(m'\omega_r\mp\omega_1)}\right\}\right]I^{\pm}I^{\mp}S_Z\equiv C_{PMZ/MPZ}\left(t\right)I^{\pm}I^{\mp}S_Z$

Table 3: Description of higher order terms appearing in the derivation of the operators $\overline{H}$ and $P\left(t\right)$ based on Method-I (bimodal formalism with $P\left(0\right)\neq1$)

Subsequently, the final form of the signal expression is derived and given below.

$$
\begin{aligned}
S(t) = Tr\left[\rho(t) S^{+}\right] = A_X(t) + \left(\frac{1}{2}\right)\left\{A_{PMX}(t) + A_{MPX}(t) + iA_{PMY}(t) + iA_{MPY}(t)\right\} \\
+ \left(\frac{1}{2}\right)\left\{C_P^*(t) + C_M(t)\right\}\left\{A_{PX}(t) + iA_{PY}(t)\right\} \\
+ \left(\frac{1}{2}\right)\left\{C_M^*(t) + C_P(t)\right\}\left\{A_{MX}(t) + iA_{MY}(t)\right\} \\
+ \left(\frac{1}{4}\right)\left\{C_{PZ}^*(t) - C_{MZ}(t)\right\}\left\{A_{PX}(t) + iA_{PY}(t)\right\} \\
+ \left(\frac{1}{4}\right)\left\{C_{MZ}^*(t) - C_{PZ}(t)\right\}\left\{A_{MX}(t) + iA_{MY}(t)\right\}
\end{aligned}
\tag{20}
$$

The coefficients $A(0)$ and $A(t)$ are described in Table 4.

Operator	**Coefficient**
S_X	$A_X(0) = 1$ $A_X(t) = \cos\left(\frac{\tilde{\omega}_{IS}^{(Z)} t}{2}\right)$
$I_Z S_Y$	$A_{ZY}(0) = 0$ $A_{ZY}(t) = 2\sin\left(\frac{\tilde{\omega}_{IS}^{(Z)} t}{2}\right)$
$I^+ S_X$	$A_{PX}(0) = C_M^*(0) + C_P(0) - \left(\frac{1}{4}\right) C_{MZ}^*(0) C_{MPZ}(0) - \left(\frac{1}{4}\right) C_{PMZ}^*(0) C_{PZ}(0)$ $A_{PX}(t) = A_{PX}(0) e^{-i\tilde{\omega}_I^{(Z)} t}$
$I^- S_X$	$A_{MX}(0) = C_P^*(0) + C_M(0) - \left(\frac{1}{4}\right) C_{PZ}^*(0) C_{PMZ}(0) - \left(\frac{1}{4}\right) C_{MPZ}^*(0) C_{MZ}(0)$ $A_{MX}(t) = A_{MX}(0) e^{+i\tilde{\omega}_I^{(Z)} t}$
$I^+ S_Y$	$A_{PY}(0) = \left(\frac{i}{2}\right)\left[C_{MZ}^*(0) - C_{PZ}(0) - C_M^*(0) C_{MPZ}(0) + C_{PMZ}^*(0) C_P(0)\right]$ $A_{PY}(t) = A_{PY}(0) e^{-i\tilde{\omega}_I^{(Z)} t}$
$I^- S_Y$	$A_{MY}(0) = \left(\frac{i}{2}\right)\left[C_{PZ}^*(0) - C_{MZ}(0) - C_P^*(0) C_{PMZ}(0) + C_{MPZ}^*(0) C_M(0)\right]$ $A_{MY}(t) = A_{MY}(0) e^{+i\tilde{\omega}_I^{(Z)} t}$
$I^+ I^- S_X$	$A_{PMX}(0) = C_M^*(0) C_M(0) - \left(\frac{1}{4}\right) C_{MZ}^*(0) C_{MZ}(0) - \left(\frac{1}{4}\right) C_{PMZ}^*(0) C_{PMZ}(0)$ $A_{PMX}(t) = A_{PMX}(0)\cos\left(\frac{\tilde{\omega}_{IS}^{(Z)} t}{2}\right) - A_{PMY}(0)\sin\left(\frac{\tilde{\omega}_{IS}^{(Z)} t}{2}\right)$
$I^- I^+ S_X$	$A_{MPX}(0) = C_P^*(0) C_P(0) - \left(\frac{1}{4}\right) C_{PZ}^*(0) C_{PZ}(0) - \left(\frac{1}{4}\right) C_{MPZ}^*(0) C_{MPZ}(0)$ $A_{MPX}(t) = A_{MPX}(0)\cos\left(\frac{\tilde{\omega}_{IS}^{(Z)} t}{2}\right) + A_{MPY}(0)\sin\left(\frac{\tilde{\omega}_{IS}^{(Z)} t}{2}\right)$
$I^+ I^- S_Y$	$A_{PMY}(0) = \left(\frac{i}{2}\right)\left[C_{PMZ}^*(0) - C_{PMZ}(0) - C_M^*(0) C_{MZ}(0) + C_{MZ}^*(0) C_M(0)\right]$ $A_{PMY}(t) = A_{PMY}(0)\cos\left(\frac{\tilde{\omega}_{IS}^{(Z)} t}{2}\right) + A_{PMX}(0)\sin\left(\frac{\tilde{\omega}_{IS}^{(Z)} t}{2}\right)$
$I^- I^+ S_Y$	$A_{MPY}(0) = \left(\frac{i}{2}\right)\left[C_{MPZ}^*(0) - C_{MPZ}(0) - C_P^*(0) C_{PZ}(0) + C_{PZ}^*(0) C_P(0)\right]$ $A_{MPY}(t) = A_{MPY}(0)\cos\left(\frac{\tilde{\omega}_{IS}^{(Z)} t}{2}\right) - A_{MPX}(0)\sin\left(\frac{\tilde{\omega}_{IS}^{(Z)} t}{2}\right)$

Table 4: Description of coefficients appearing in the derivation of the signal expression (Eqns.(19) and (20)) based on Method-I (bimodal formalism) with $P(0) \neq 1$

Part-B (Method-II)

B1. Time evolution in the Schrödinger picture

Owing to the similar form of the operator $\overline{H}$ in both Method-I and Method-II, the diagonalization transformation leads to a similar form of the transformed operator, $\overline{H_d}$ (with $\overline{H_d} = U_1 \overline{H} U_1^\dagger$).

$$U_{\alpha\beta} = e^{i\theta_\beta I_X S_\beta} e^{i\theta_\alpha I_X S_\alpha} \tag{21}$$

$$\tan\theta_{\alpha/\beta} = \frac{\left(\omega_I^{(Y)} \pm 2\omega_{IS}^{(Y)}\right)}{\omega_I^{(Z)}} \tag{22}$$

$$\overline{H'} = U_{\alpha\beta} \overline{H} U_{\alpha\beta}^\dagger = \tilde{\omega}_I^{(Z)} I_Z + \tilde{\omega}_{IS}^{(Z)} I_Z S_Z \tag{23}$$

The coefficients $\tilde{\omega}_I^{(Z)}/\tilde{\omega}_{IS}^{(Z)}$ are defined in terms of the original ω-coefficients in the operator $\overline{H}$ (Eq.(100) of the main section).

$$\tilde{\omega}_I^{(Z)} = -\left[\left(\frac{\omega_I^{(Z)}}{2}\right)^2 + \left(\frac{\omega_I^{(Y)}}{2} + \omega_{IS}^{(Y)}\right)^2\right]^{1/2} - \left[\left(\frac{\omega_I^{(Z)}}{2}\right)^2 + \left(\frac{\omega_I^{(Y)}}{2} - \omega_{IS}^{(Y)}\right)^2\right]^{1/2} \tag{24}$$

$$\tilde{\omega}_{IS}^{(Z)} = -\left(\frac{1}{2}\right)\left[\left(\frac{\omega_I^{(Z)}}{2}\right)^2 + \left(\frac{\omega_I^{(Y)}}{2} + \omega_{IS}^{(Y)}\right)^2\right]^{1/2} + \left(\frac{1}{2}\right)\left[\left(\frac{\omega_I^{(Z)}}{2}\right)^2 + \left(\frac{\omega_I^{(Y)}}{2} - \omega_{IS}^{(Y)}\right)^2\right]^{1/2} \tag{25}$$

To maintain consistency, both the initial density operator ($\rho(0) = S_X$), the operator, $P(t)$ and the detection operator, S^+ are also transformed as follows.

$$\rho_d(0) = U_1 \rho(0) U_1^\dagger = S_X \cos\left(\frac{\theta_\alpha - \theta_\beta}{2}\right) - 2I_X S_Y \sin\left(\frac{\theta_\alpha - \theta_\beta}{2}\right) \tag{26}$$

$$\Lambda_d(t) = U_1 \Lambda(t) U_1^\dagger \simeq \Lambda(t) \tag{27}$$

$$S_d^+ = S^+ \cos\left(\frac{\theta_\alpha - \theta_\beta}{2}\right) + 2iI_X S^+ \sin\left(\frac{\theta_\alpha - \theta_\beta}{2}\right) \tag{28}$$

where we have retained the corrections due to the transformations for the operator $\Lambda(t)$ to the lowest order.

Employing the above relations, the time-domain signal can be derived through suitable approximations as follows.

$$\rho_d(t) = U_d(t)\,\rho_d(0)\,U_d^\dagger(t) = e^{-i\Lambda_d(t)} \underbrace{e^{-i\overline{H_d}t} \rho_d(0) e^{i\overline{H_d}t}}_{\rho_d'(t)} e^{i\Lambda_d(t)} \tag{29}$$

where, $U_d(t) = U_1 U(t) U_1^\dagger = P_d(t) e^{-i\overline{H_d}t}$, represents the transformed evolution operator.

By employing the form of $\overline{H_d}$ given above, the form for $\rho_d'(t)$ can be derived as follows.

$$\rho_d'(t) = \cos\left(\frac{\theta_\alpha - \theta_\beta}{2}\right)\left\{S_X \cos\left(\frac{\tilde{\omega}_{IS}^{(Z)} t}{2}\right) + 2I_Z S_Y \sin\left(\frac{\tilde{\omega}_{IS}^{(Z)} t}{2}\right)\right\}$$
$$- 2\sin\left(\frac{\theta_\alpha - \theta_\beta}{2}\right)\left\{I_X S_Y \cos\left(\tilde{\omega}_I^{(Z)} t\right) + I_Y S_Y \sin\left(\tilde{\omega}_I^{(Z)} t\right)\right\} \tag{30}$$

This leads to the following form for the signal expression:

$$S(t) = Tr\left[\rho_d(t) S_d^+\right] = \widetilde{C}_1(t).\cos\left(\frac{\tilde{\omega}_{IS}^{(Z)}t}{2}\right) + \widetilde{S}_1(t).\sin\left(\frac{\tilde{\omega}_{IS}^{(Z)}t}{2}\right)$$
$$+ \widetilde{C}_2(t).\cos\left(\tilde{\omega}_I^{(Z)}t\right) + \widetilde{S}_2(t).\sin\left(\tilde{\omega}_I^{(Z)}t\right) \quad (31)$$

where the coefficients $\widetilde{C}_i(t)/\widetilde{S}_i(t)$ are defined in Table 5.

CW Decoupling Method-I	**Signal Coefficient**
$\widetilde{C}_1(t)$	$\left\{1-\frac{1}{8}\left(\widetilde{C}_{XZ}^2(t)-\widetilde{C}_{YZ}^2(t)\right)\right\}\cos^2\left(\frac{\theta_\alpha-\theta_\beta}{2}\right)-\left\{\frac{1}{4}\widetilde{C}_{XZ}(t)\right\}\sin(\theta_\alpha-\theta_\beta)$
$\widetilde{S}_1(t)$	$-\left\{\frac{1}{2}\widetilde{C}_Y(t)\right\}\sin(\theta_\alpha-\theta_\beta)-\left\{\frac{1}{4}\left(\widetilde{C}_Y(t)\,\widetilde{C}_{XZ}(t)-\widetilde{C}_X(t)\,\widetilde{C}_{YZ}(t)\right)\right\}\cos^2\left(\frac{\theta_\alpha-\theta_\beta}{2}\right)$
$\widetilde{C}_2(t)$	$\left\{1+\frac{1}{2}\widetilde{C}_Y^2(t)+\frac{1}{8}\widetilde{C}_{XZ}^2(t)\right\}\sin^2\left(\frac{\theta_\alpha-\theta_\beta}{2}\right)-\left\{\frac{1}{4}\widetilde{C}_{XZ}(t)\right\}\sin(\theta_\alpha-\theta_\beta)$
$\widetilde{S}_2(t)$	$-\left\{\frac{1}{2}\tilde{C}_Y(t)\,\tilde{C}_X(t)+\frac{1}{8}\tilde{C}_{YZ}(t)\,\tilde{C}_{XZ}(t)\right\}\sin^2\left(\frac{\theta_\alpha-\theta_\beta}{2}\right)-\left\{\frac{1}{2}\tilde{C}_Y(t)\right\}\sin(\theta_\alpha-\theta_\beta)$

Table 5: Description of coefficients ($C_i(t)$ and $S_i(t)$) appearing in the derivation of the time-domain signal (Eq.(31)) based on Method-II (Schrödinger picture formalism)

Role of non-secular terms in time evolution

Analogous to the discussion in Part-A, to rule out the role of the non-secular terms (such $[\mathcal{H}_0, \mathcal{H}_n]]$) in $\overline{H}$ in the discrepancy observed in the analytic simulations in the Schrodinger picture, additional simulations, both in the presence and absence of the non-secular terms were performed and compared with numerical simulations. As indicated in Figure 2, the analytic simulations both in the presence (first row, indicated in red color) and absence (second row, indicated in blue color) are in complete disagreement to those obtained from numerical simulations (indicated in black color). Hence, the disagreement observed in the analytic simulations could be due to some inherent limitations of the method.

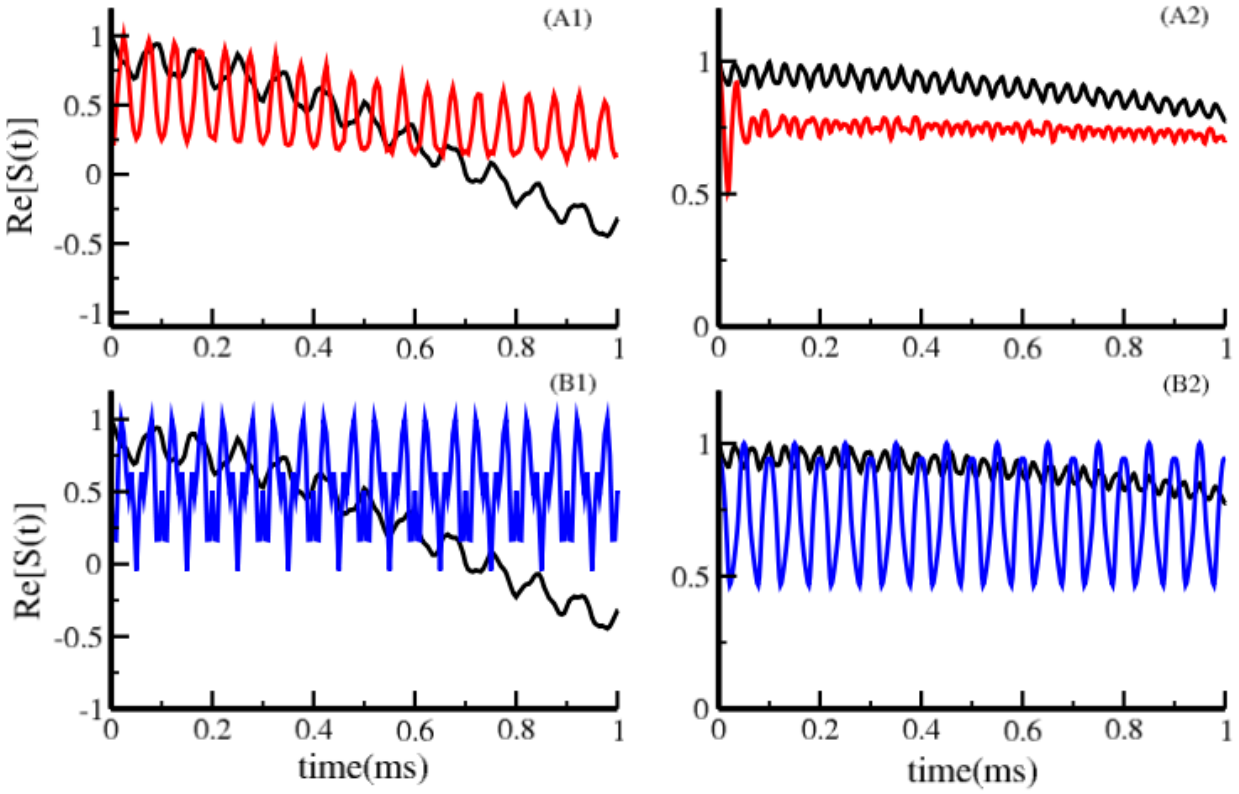

Figure 2: In the simulations depicted, the time-domain signal (panels A1-A2 and B1-B2) under CW decoupling is illustrated under varying RF amplitudes (i.e. $\nu_r = 20\,\text{kHz}$; $\nu_1 = 50\,\text{kHz}$ (panels A1, B1) and $\nu_1 = 50\,\text{kHz}$; $\nu_1 = 20\,\text{kHz}$ (panels A2, B2)). The simulations from numerical methods (indicated through black solid line) are compared with analytic simulations based on **single-mode** based Method-II formalism with i) complete form of $\overline{H}$ (indicated in red, top row) and ii) with non-secular terms dropped from $\overline{H}$ (indicated in blue, bottom row). All other parameters are similar to those employed in the main article.

B2. Time evolution in the Interaction picture

(i) Normal boundary condition ($P(0) = 1$)

Based on the calculations given in the main section, the final form of the signal expression in the interaction picture is given by the following equation.

$$S(t) = Tr\left[\rho(t) S^{+}\right] = \widetilde{C}_1(t) \cos\left(\frac{\tilde{\omega}_{IS}^{(Z)} t}{2}\right) + \widetilde{S}_1(t) \sin\left(\frac{\tilde{\omega}_{IS}^{(Z)} t}{2}\right) \tag{32}$$

where the coefficients $C_i(t)/S_i(t)$ are defined in Table 6.

CW Decoupling Method-I	**Signal Coefficient**
$\widetilde{C}_1(t)$	$\left[1 - \frac{1}{2}\left\{\frac{1}{2}\widetilde{C}_{PZ}(t)\,\widetilde{C}_{MZ}(t) + \frac{1}{8}\widetilde{C}_{ZZ}^{2}(t)\right\}\right]$
$\widetilde{S}_1(t)$	$\left[\frac{1}{4}\widetilde{C}_{ZZ}(t)\right]$

Table 6: Description of coefficients ($C_i(t)$ and $S_i(t)$) appearing in the derivation of the time-domain signal (Eq.(96) of the main article) based on Method-II (Interaction picture formalism)

(ii) Alternate boundary condition ($P(0) \neq 1$)

Employing bimodal FME formalism, the evolution operator in the standard Hilbert space is derived in terms of the operators $\overline{H}$ and $\Lambda(t)$, as given below.

$$U(t) = e^{-i\Lambda(t)} e^{-i\overline{H}t} e^{i\Lambda(0)} \tag{33}$$

$$\overline{H} = \bar{H}^{(1)} + \bar{H}^{(2)} = \underbrace{\tilde{\omega}_{I}^{(Z)} I_Z + \tilde{\omega}_{IS}^{(Z)} I_Z S_Z}_{\bar{H}^{(2)}} \tag{34}$$

$$\Lambda(t) = \Lambda_1(t) + \Lambda_2(t) = \underbrace{\widetilde{C}_P(t) I^{+} + \widetilde{C}_M(t) I^{-} + \widetilde{C}_{PZ}(t) I^{+} S_Z + \widetilde{C}_{MZ}(t) I^{-} S_Z}_{\Lambda_1(t)}$$
$$+ \underbrace{\widetilde{C}_Z(t) I_Z + \widetilde{C}_{ZZ}(t) I_Z S_Z}_{\Lambda_2(t)} \tag{35}$$

A detailed description of the various cross-terms employed in the derivation of the effective evolution operator is listed in Table 7.

Subsequently, utilizing the modified form of $U(t)$, the evolution of the system under CW decoupling is calculated and given below.

$$\rho(t) = U(t)\,\rho(t)\,U^{\dagger}(t) = e^{-i\Lambda(t)} e^{-i\overline{H}t} e^{i\Lambda(0)} \rho(0)\, e^{-i\Lambda(0)} e^{i\overline{H}t} e^{i\Lambda(t)} \tag{36}$$

Cross-Term (CW Decoupling)	**Method-II (bimodal)**	**Method-II (bimodal)**
Operator	$\overline{H}$	$\mathbf{\Lambda\,(t)}$
$\mathrm{H_I}$	-	$\left\{\sum\limits_{m=-2}^{2}\left(\frac{i\omega_I^{(m)}}{2(m\omega_r\pm\omega_1)}\right)\left(e^{i(m\omega_r\pm\omega_1)t}\right)\right\}I^{\pm}\equiv\widetilde{C}_{P/M}\,(t)\,I^{\pm}$
$\mathrm{H_{IS}}$	-	$\left\{\sum\limits_{\substack{m=-2\\m\neq0}}^{2}\left(\frac{i\omega_{IS}^{(m)}}{(m\omega_r\pm\omega_1)}\right)\left(e^{i(m\omega_r\pm\omega_1)t}\right)\right\}I^{\pm}S_Z\equiv\widetilde{C}_{PZ/MZ}\,(t)\,I^{\pm}S_Z$
$\mathrm{H_I}\times\mathrm{H_I}$	$-\frac{1}{2}\left\{\sum\limits_{m=-2}^{2}\frac{\left\lvert\omega_I^{(m)}\right\rvert^2\omega_1}{\left(m^2\omega_r^2-\omega_1^2\right)}\right\}I_Z\equiv\omega_I^{(Z)}I_Z$	$\left(\frac{i}{4}\right)\left[\sum\limits_{m,m'=-2}^{2}\omega_I^{(m)}\omega_I^{(m')}\left\{\left(\frac{e^{i(m+m')\omega_r t}}{(m+m')\omega_r}\right)\left(\frac{2\omega_1}{\left(m^2\omega_r^2-\omega_1^2\right)}\right)\right\}\right]I_Z\equiv\widetilde{C}_Z\,(t)\,I_Z$
$\mathrm{H_{IS}}\times\mathrm{H_{IS}}$	$-\frac{1}{2}\left\{\sum\limits_{\substack{m=-2\\m\neq0}}^{2}\frac{\left\lvert\omega_{IS}^{(m)}\right\rvert^2\omega_1}{\left(m^2\omega_r^2-\omega_1^2\right)}\right\}I_Z\equiv\omega_I^{(Z)}I_Z$	$\left(\frac{i}{4}\right)\left[\sum\limits_{m,m'=-2}^{2}\omega_{IS}^{(m)}\omega_{IS}^{(m')}\left\{\left(\frac{e^{i(m+m')\omega_r t}}{(m+m')\omega_r}\right)\left(\frac{2\omega_1}{\left(m^2\omega_r^2-\omega_1^2\right)}\right)\right\}\right]I_Z\equiv\widetilde{C}_Z\,(t)\,I_Z$
$\mathrm{H_I}\times\mathrm{H_{IS}}$	$-\left\{\sum\limits_{m=-2}^{2}\left(\omega_I^{(m)}\omega_{IS}^{(-m)}+\omega_{IS}^{(m)}\omega_I^{(-m)}\right)\underbrace{\frac{\omega_1}{\left(m^2\omega_r^2-\omega_1^2\right)}}_{\text{ResDip}}\right\}I_ZS_Z$ $\equiv\omega_{IS}^{(Z)}I_ZS_Z$	$\left(\frac{i}{2}\right)\left[\sum\limits_{m,m'=-2}^{2}\left(\omega_I^{(m)}\omega_{IS}^{(m')}+\omega_{IS}^{(m)}\omega_I^{(m')}\right)\left\{\left(\frac{e^{i(m+m')\omega_r t}}{(m+m')\omega_r}\right)\left(\frac{2\omega_1}{\left(m^2\omega_r^2-\omega_1^2\right)}\right)\right\}\right]I_ZS_Z$ $\equiv\widetilde{C}_{ZZ}\,(t)\,I_ZS_Z$

Table 7: Description of higher order terms appearing in the derivation of $\overline{H}$ and $\Lambda\,(t)$ based on Method-II (bimodal formalism with $\Lambda\,(0)\neq0$)

$$\rho(t) = e^{-i\Lambda(t)} \underbrace{e^{-i\overline{H}t} e^{i\Lambda(0)} \rho(0) e^{-i\Lambda(0)} e^{i\overline{H}t}}_{\tilde{\rho}_0(t)} e^{i\Lambda(t)} = \tilde{\rho}_0(t) + \{-i[\Lambda(t), \tilde{\rho}_0(t)]\} \tag{37}$$

$$\tilde{\rho}_0(0) = e^{i\Lambda(0)} \rho(0) e^{-i\Lambda(0)} = \rho(0) + i[\Lambda(0), \rho(0)] \tag{38}$$

$$\begin{aligned} S(t) &= Tr\left[\rho(t) S^{+}\right] \\ &= \left[\cos\left(\frac{\tilde{\omega}_{IS}^{(Z)} t}{2}\right) + \frac{1}{2}\widetilde{C}_{ZZ}(0) \sin\left(\frac{\tilde{\omega}_{IS}^{(Z)} t}{2}\right)\right] \\ &+ \frac{1}{2}\left[\widetilde{C}_{PZ}(t) \widetilde{C}_{MZ}(0) e^{i\tilde{\omega}_{I}^{(Z)} t} + \widetilde{C}_{MZ}(t) \widetilde{C}_{PZ}(0) e^{-i\tilde{\omega}_{I}^{(Z)} t}\right] \end{aligned} \tag{39}$$

Part-C (Method-III)

C1. Time evolution in the Schrödinger picture

In order to employ Floquet theory, the time-dependent Hamiltonian in the tilted rotating frame (Eqns.(20)-(23)) is transformed into a time-independent Floquet Hamiltonian.

$$H_F = \omega_r I_F + H_{F,I}^{CSA} + H_{F,IS} + H_{F,I}^{CW} \tag{40}$$

$$H_{F,I}^{CW} = \omega_1 [I_Z]_0 = \left(G^Z\right)_I^{(0)} [I_Z]_0 \tag{41}$$

$$H_{F,I}^{CSA} = -\Delta\omega [I_X]_0 - \sum_{\substack{m=-2 \\ m\neq 0}}^{2} \omega_I^{(m)} [I_X]_m = \sum_{m=-2}^{2} \left\{ \left(G^+\right)_I^{(m)} \left[I^+\right]_m + \left(G^-\right)_I^{(m)} \left[I^-\right]_m \right\} \tag{42}$$

$$H_{F,IS} = -\sum_{\substack{m=-2 \\ m\neq 0}}^{2} 2\omega_{IS}^{(m)} [I_X S_Z]_m = \sum_{\substack{m=-2 \\ m\neq 0}}^{2} \left\{ \left(G^+\right)_{IS}^{(m)} \left[I^+ S_Z\right]_m + \left(G^-\right)_{IS}^{(m)} \left[I^- S_Z\right]_m \right\} \tag{43}$$

The above expressions lead to the introduction of the so-called "dressed states" ($|\Phi_M; n\rangle$) and "ladder operators" (F_n) belonging to an extended Hilbert space. The basis states in the extended space are constructed from a direct product between the spin states (defined in the Hilbert space) with those of the Fourier states (defined in the Fourier space). The spin Hamiltonian operators ($\left[\hat{A}\right]_n$), in the extended Hilbert space are constructed from a direct product between the Fourier operator, F_n (defined in an infinite dimensional vector space) and the spin operator, $\hat{A}$ (defined in a finite dimensional vector space):

$$|\Phi_\alpha; m\rangle = |n\rangle \otimes |\Phi_\alpha\rangle \quad ; \quad \hat{A}_n = F_n \otimes \hat{A} \tag{44}$$

The number operator, I_F corresponding to the MAS modulation in the extended Hilbert space is defined as in the infinite dimensional Fourier space in the following manner.

$$I_F = \sum_{m=-\infty}^{\infty} \{m\, |m\rangle \langle m|\} \tag{45}$$

The details of the infinite dimensional extended Hilbert spaces can be found in references [3], [4] and [16] mentioned in the main article.

To simplify the description in the extended Hilbert space, contact transformation is employed to derive an effective Hamiltonian. Accordingly, the Floquet Hamiltonian is represented in terms of a zero-order and perturbing Floquet Hamiltonian as defined below:

$$H_0 = \omega_r I_F + H_{F,I}^{CW} \tag{46}$$

$$H_1 = H_{F,I}^{CSA} + H_{F,IS} \tag{47}$$

Employing the transformation function S_1 (Table 8), the Floquet Hamiltonian is transformed, resulting in an effective Hamiltonian (H_F^{eff}).

$$S_1 = i\left[S_{1,I} + S_{1,IS}\right] \tag{48}$$

$$H_F^{eff} = e^{i\lambda S_1} H_F e^{-i\lambda S_1} = H_0 + H_{2,d}^{(1)} = \omega_r I_F + \widetilde{\omega}_I [I_Z]_0 + \widetilde{\omega}_{IS} [I_Z S_Z]_0 \tag{49}$$

The coefficients in the effective Hamiltonian (Eq.(8)) are similar to those derived using FME (Table VII of main article).

Operator	**Coefficients**
1. Hamiltonian	
$\mathbf{H_{F,I}}$	
$[I^{\pm}]_0$	$(G^{\pm})_I^{(0)} = -\frac{\Delta\omega}{2}$
$[I^{\pm}]_m$	$(G^{\pm})_I^{(m)} = -\frac{\omega_I^{(m)}}{2}$
$[I_Z]_0$	$\left(G^Z\right)_I^{(0)} = \omega_1$
$\mathbf{H_{F,IS}}$	
$[I^{\pm}S_Z]_m$	$(G^{\pm})_{IS}^{(m)} = -\omega_{IS}^{(m)}$
2. Transformation function	
Single spin operators	
$\mathbf{S_{1,I}}$	
$[I^{\pm}]_m$	$(C^{\pm})_I^{(m)} = \frac{-i\left(G^{\pm}\right)_I^{(m)}}{(m\omega_r \pm \omega_1)}$
Two spin operators	
$\mathbf{S_{1,IS}}$	
$[I^{\pm}S_Z]_{m,}$	$(C^{\pm})_{IS}^{(m)} = \frac{-i\left(G^{\pm}\right)_{IS}^{(m)}}{(m\omega_r \pm \omega_1)}$

Table 8: Description of coefficients present in the Floquet Hamiltonian and the transformation functions (S_1) employed in contact transformation methods (single mode)

To have a consistent description, both the initial density operator ($\rho_F(0) = [S_X]_{0,0}$) and the detection operator ($[S^+]_{0,0}$) are transformed by the transformation function, S_1,

$$\tilde{\rho}_F(0) = e^{i\lambda S_1}\rho_F(0)\,e^{-i\lambda S_1} \tag{50}$$

$$\tilde{S}^+ = e^{i\lambda S_1}\left[S^+\right]_{0,0}e^{-i\lambda S_1} \tag{51}$$

Subsequently, the time domain signal in the Floquet framework is evaluated,

$$\begin{aligned}\left\langle \tilde{S}^+(t)\right\rangle_F &= Tr\left[\tilde{\rho}_F(t)\,\tilde{S}^+\right] = \left[A^2 - B^2\right]\cos\left(\frac{\tilde{\omega}_{IS}^{(1)}t}{2}\right)\\ &+ \sum_{\substack{m=-2\\ m\neq 0}}^{2}\left\{\frac{\left|\omega_{IS}^{(m)}\right|^2}{\left(m\omega_r+\omega_1\right)^2}e^{i(\tilde{\omega}_I+m\omega_r+\omega_1)t} + \frac{\left|\omega_{IS}^{(m)}\right|^2}{\left(m\omega_r-\omega_1\right)^2}e^{i(-\tilde{\omega}_I+m\omega_r-\omega_1)t}\right\}\end{aligned} \tag{52}$$

where, $\tilde{\rho}_F(t) = e^{-iH_{F,CT}^{eff}t}\tilde{\rho}_F(0)\,e^{iH_{F,CT}^{eff}t}$. In the above expression, the coefficients A and B have the following definitions:

$$A = \left(1 - \frac{1}{2}\sum_{\substack{m=-2\\ m\neq 0}}^{2}\left|\omega_{IS}^{(m)}\right|^2\frac{m^2\omega_r^2+\omega_1^2}{\left(m^2\omega_r^2-\omega_1^2\right)^2}\right) \quad ; \quad B = \sum_{m=-2}^{2}\frac{m\omega_r\omega_1\omega_I^{(m)}\omega_{IS}^{(-m)}}{\left(m^2\omega_r^2-\omega_1^2\right)^2} \tag{53}$$

C2. Time evolution in the Interaction picture

Employing an operator basis defined in an infinite dimensional vector space, the time-dependent Hamiltonian in the RF interaction frame (Eqns.(44)-(46)) is transformed into a time-independent Floquet Hamiltonian.

$$H_F = \omega_r I_F + \omega_1 S_F + H_{F,I} + H_{F,IS} \tag{54}$$

where

$$H_{F,I} = \sum_{m=-2}^{2}\left\{\left(G^+\right)_I^{(m,+1)}\left[I^+\right]_{m,+1} + \left(G^-\right)_I^{(m,-1)}\left[I^-\right]_{m,-1}\right\} \tag{55}$$

$$H_{F,IS} = \sum_{\substack{m=-2\\ m\neq 0}}^{2}\left\{\left(G^+\right)_{IS}^{(m,+1)}\left[I^+S_Z\right]_{m,+1} + \left(G^-\right)_{IS}^{(m,-1)}\left[I^-S_Z\right]_{m,-1}\right\} \tag{56}$$

A detailed description of the Floquet operators (I_F, S_F, $(O_p)_{m,n}$) is well-documented and is omitted to avoid repetition. The 'G' coefficients employed in the Floquet Hamiltonian are given in Table 9. The time-independent Floquet Hamiltonian is defined in an infinite dimensional vector space and in its present form is less suited for analytic description. To alleviate this problem in the Floquet-Hilbert space, perturbative approaches based on contact transformation is employed to derive effective Floquet Hamiltonians.

In accord with perturbative treatments, the Floquet Hamiltonian is split and re-expressed as a sum of zero-order and perturbing Hamiltonians:

$$H_0 = \omega_r I_F + \omega_1 S_F \tag{57}$$

$$H_1 = H_{F,I} + H_{F,IS} \tag{58}$$

Operator	Coefficients
1. Hamiltonian	
$\mathbf{H_{F,I}}$	
$[I^{\pm}]_{0,\pm1}$	$(G^{\pm})_{I}^{(0,\pm1)} = -\frac{\Delta\omega}{2}$
$[I^{\pm}]_{m,\pm1}$	$(G^{\pm})_{I}^{(m,\pm1)} = -\frac{\omega_I^{(m)}}{2}$
$\mathbf{H_{F,IS}}$	
$[I^{\pm}S_Z]_{m,\pm1}$	$(G^{\pm})_{IS}^{(m,\pm1)} = -\omega_{IS}^{(m)}$
2. Transformation function	
Single spin operators	
$\mathbf{S_{1,I}}$	
$[I^{\pm}]_{m,\pm1}$	$(C^{\pm})_{I}^{(m,\pm1)} = \frac{-i\left(G^{\pm}\right)_{I}^{(m,\pm1)}}{(m\omega_r \pm \omega_1)}$
Two spin operators	
$\mathbf{S_{1,IS}}$	
$[I^{\pm}S_Z]_{m,\pm1}$	$(C^{\pm})_{I}^{(m,\pm1)} = \frac{-i\left(G^{\pm}\right)_{IS}^{(m,\pm1)}}{(m\omega_r \pm \omega_1)}$

Table 9: Description of coefficients present in the Floquet Hamiltonian and the transformation functions (S_1) employed in contact transformation methods (bimodal)

The zero order Hamiltonian (H_0) mostly comprises of operators that are diagonal in the Fourier dimension, while, the perturbing Hamiltonian (H_1) comprises of operators that are off-diagonal in the Fourier dimension.

Employing the transformation function, S_1, the original Floquet Hamiltonian is transformed into an effective Hamiltonian:

$$H_{F,CT}^{eff} = e^{i\lambda S_1} H_F e^{-i\lambda S_1} \tag{59}$$

The transformation function 'S_1' comprises of operators, whose coefficients are chosen to compensate the off-diagonality to order 'λ' in H_1 (i.e. $H_1^{(1)} = H_1 + i\left[S_1, H_0\right] = 0$):

$$S_1 = i\left[S_{1,I} + S_{1,IS}\right] \tag{60}$$

A detailed description of the operators is S_1, along with their coefficients $(C^{+})_{I/IS}^{(m,n)}$ and $(C^{-})_{I/IS}^{(m,n)}$ is listed in Table 9.

Subsequently, following the standard procedure, the effective Hamiltonian (upto second order) is derived and expressed in terms of operators that are diagonal in both the spin and Fourier dimension.

$$H_{F,CT}^{eff} = H_0 + H_{2,d}^{(1)} = \omega_r I_F + \omega_1 S_F + \tilde{\omega}_I [I_Z]_{0,0} + \tilde{\omega}_{IS} [I_Z S_Z]_{0,0} \tag{61}$$

Subsequently, the time domain signal in the Floquet framework is evaluated,

$$\left\langle \tilde{S}^{+}\left(t\right)\right\rangle_{F} = Tr\left[\tilde{\rho}_{F}\left(t\right)\tilde{S}^{+}\right] = \left[A^{2}-B^{2}\right]\cos\left(\frac{\tilde{\omega}_{IS}^{(1)}t}{2}\right) + \sum_{\substack{m=-2\\ m\neq 0}}^{2}\left\{\frac{\left|\omega_{IS}^{(m)}\right|^{2}}{\left(m\omega_{r}+\omega_{1}\right)^{2}}e^{i(\tilde{\omega}_{I}+m\omega_{r}+\omega_{1})t} + \frac{\left|\omega_{IS}^{(m)}\right|^{2}}{\left(m\omega_{r}-\omega_{1}\right)^{2}}e^{i(-\tilde{\omega}_{I}+m\omega_{r}-\omega_{1})t}\right\} \tag{62}$$

where, $\tilde{\rho}_{F}\left(t\right) = e^{-iH_{F,CT}^{eff}t}\tilde{\rho}_{F}\left(0\right)e^{iH_{F,CT}^{eff}t}$. In the above expression, the coefficients A and B are defined exactly as in Eq.(12).

Thus, both single and bimodal formulations of Floquet theory lead to similar signal expressions, thus proving their equivalence in the analysis of the time-evolution problem.

C3. Role of higher order corrections in contact transformation based formalism

In Figure 3, analytic simulations emerging from Floquet theory (incorporating corrections to 2nd order) are compared with numerical simulations in the top row. The differences arising thereof, especially with the amplitude of the RF field approaching the spinning frequency, can be attributed to the role of higher order corrections. In the analytic simulations in panel B1, diagonal corrections to fourth order are incorporated, while, in the analytic simulations depicted in panel B2, diagonal corrections to second order resulting from two transformations are employed to match the results obtained from numerical methods.

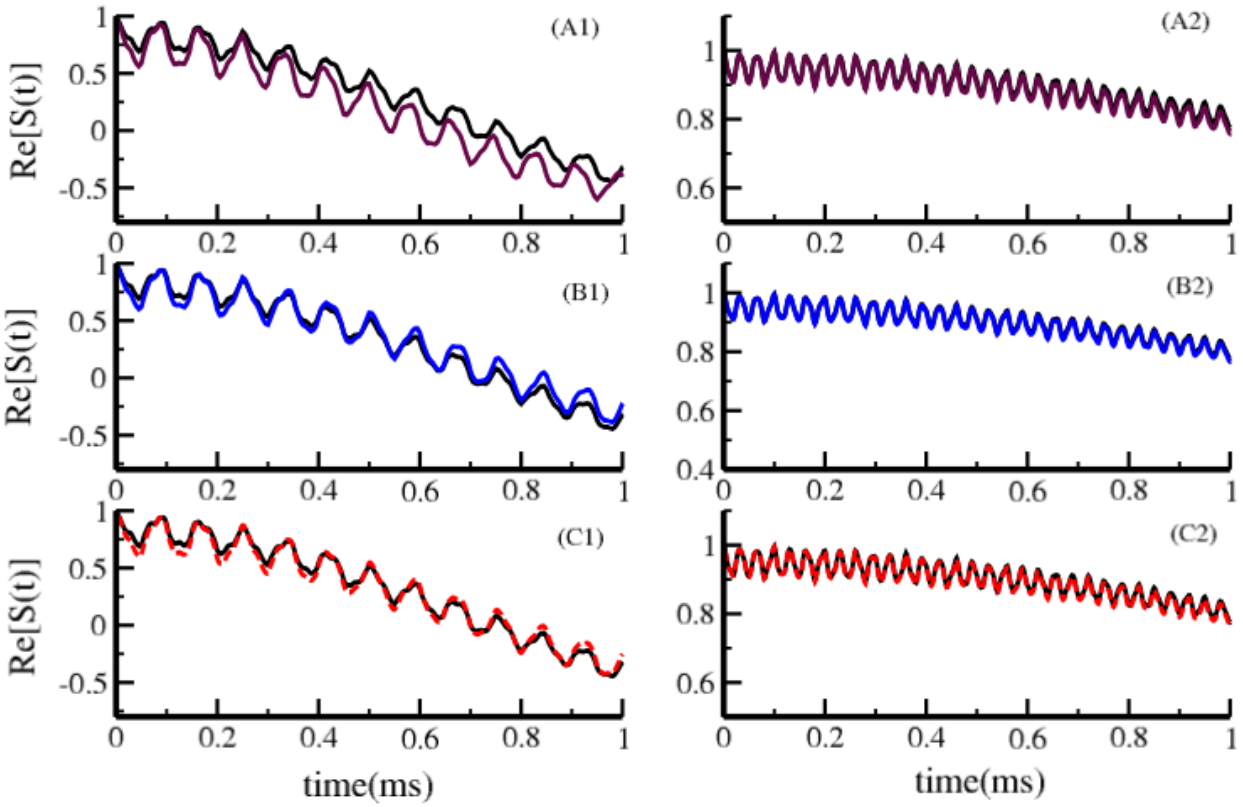

Figure 3: In the simulations depicted, the time-domain signal (panels A1-A2 and B1-B2) under CW decoupling is illustrated under varying spinning frequencies and RF amplitudes (i.e. $\nu_r = 20\,\text{kHz}$; $\nu_1 = 50\,\text{kHz}$ (panels A1, B1, C1) and $\nu_r = 50\,\text{kHz}$ $\nu_1 = 20\,\text{kHz}$ (panels A2, B2, C2)). The simulations from numerical methods (indicated through black solid line) are compared with analytic simulations based on Floquet theory with i) effective Hamiltonians incorporating corrections upto order λ^2 (indicated in maroon in panels A1, A2), ii) effective Hamiltonians incorporating corrections upto order λ^4 (indicated in blue in panels B1, B2) and order λ^2 from two transformations (indicated in red in panels C1, C2). All other parameters are similar to those employed in the simulations the main article.